

# Topological surface state transport and current saturation in topological insulator nanoribbons field effect transistors

Luis A. Jauregui<sup>1</sup>, Michael T. Pettes<sup>2</sup>, Li Shi<sup>2</sup>, Yong P. Chen<sup>1</sup>

<sup>1</sup> Purdue University, West Lafayette, IN 47907, USA <sup>2</sup> University of Texas at Austin, Austin, TX 78712

Email: jauregui@purdue.edu, Phone: (765) 496-3059, Fax: (765)494-0706

Topological insulators (TIs) are a new class of quantum matter, with an insulating bulk, where electrons on the surface behave as massless Dirac fermions as in graphene [1,2]. However, in contrast with graphene, the surface state of TIs is topologically protected against non-magnetic disorder or lattice defects. This topological protection, unique to TIs, originates from the spin locked to the Fermi momentum (“spin-helical Dirac electrons”, where backscattering is forbidden). Consequently, TI nanowire (NW) devices may outperform conventional semiconductor NWs or graphene nanoribbon (NR) devices that may suffer from backscattering. However, one of the main limitations to explore device applications in TIs was its large bulk conductance, shunting the surface conduction and also impeding effective gate tuning.

Recently, we demonstrated unambiguous transport signatures of the topological surface states Dirac fermions, such as linear energy dispersion (Fig. 1a) and  $\pi$  Berry’s phase (Fig. 1b) of our gate-tunable bulk-insulating  $\text{Bi}_2\text{Te}_3$  TINR devices, when the Fermi energy is tuned into the bulk gap [3]. Here, we report the first observation of saturating transistor characteristics in such  $\text{Bi}_2\text{Te}_3$  NR FET devices. We fabricated several FETs on  $\text{SiO}_2$  and high-k,  $\text{SrTiO}_3$ (STO) dielectric substrates (SEM image in inset of Fig. 1c). Ambipolar field effect is mainly found in TINRs devices on STO (Fig. 1c). We measured their I-V curves, and we observed  $I_{ds}$  saturates at considerably large electric fields (Fig 1d). Figure 1e depicts the extracted drift velocity ( $v_{drift} = I_{ds}L/en_{2D}W$ ) vs.  $V_{ds}$ , where L is the channel length, W is the width of the TINR, e is the electron charge and  $n_{2D}$  is the carrier density ( $n_{2D} = C_g(V_g - V_{CNP})$ ). Velocity saturation ( $v_{sat}$ ) is extracted from  $v_{drift} = ((\mu E)^{-\beta} + (v_{sat})^{\beta})^{-1/\beta}$  (where  $\mu$  is mobility, E is electric field and  $\beta$  is a fitting parameter  $\sim 1$ ) and plotted vs.  $1/E_F$  in Fig. 1f for the 2 different substrates. The  $v_{sat}$  depends on  $n_{2D}$  and we attribute this to scattering by interfacial phonons in the substrate supporting the TINR channel. The energy of the interfacial phonons ( $\hbar\Omega$ ) is extracted from the slope of  $v_{sat}$  vs.  $1/E_F$ , obtaining for TINR devices on  $\text{SiO}_2$  and on STO substrates  $\sim 60$  meV (surface phonon energy of  $\text{SiO}_2 = 55$  meV) and 120 meV respectively. This result suggests that  $v_{sat}$  of TINRs on  $\text{SiO}_2$  is mainly limited by the interfacial phonons of the substrate. However, TINRs on STO show higher  $v_{sat}$ , therefore higher current saturation. The achieved saturation current in our TINRs can be comparable or even exceed that measured previously in graphene. Our results pave the way of using TINR devices for analogue and radio-frequency circuit applications and its potential applications in topologically protected 1-D electronic devices, low-power electronics and exotic devices for topological quantum computing.

[1]Qi, X. L. *et al. Phys. Rev. B* **78**, 195424 (2008).

[2]Hasan, M. Z. & Kane, C. L. *Reviews of Modern Physics* **82**, 3045 (2010).

[3]Jauregui, L. A. *et al. arxiv: 1402.2659* (2014).

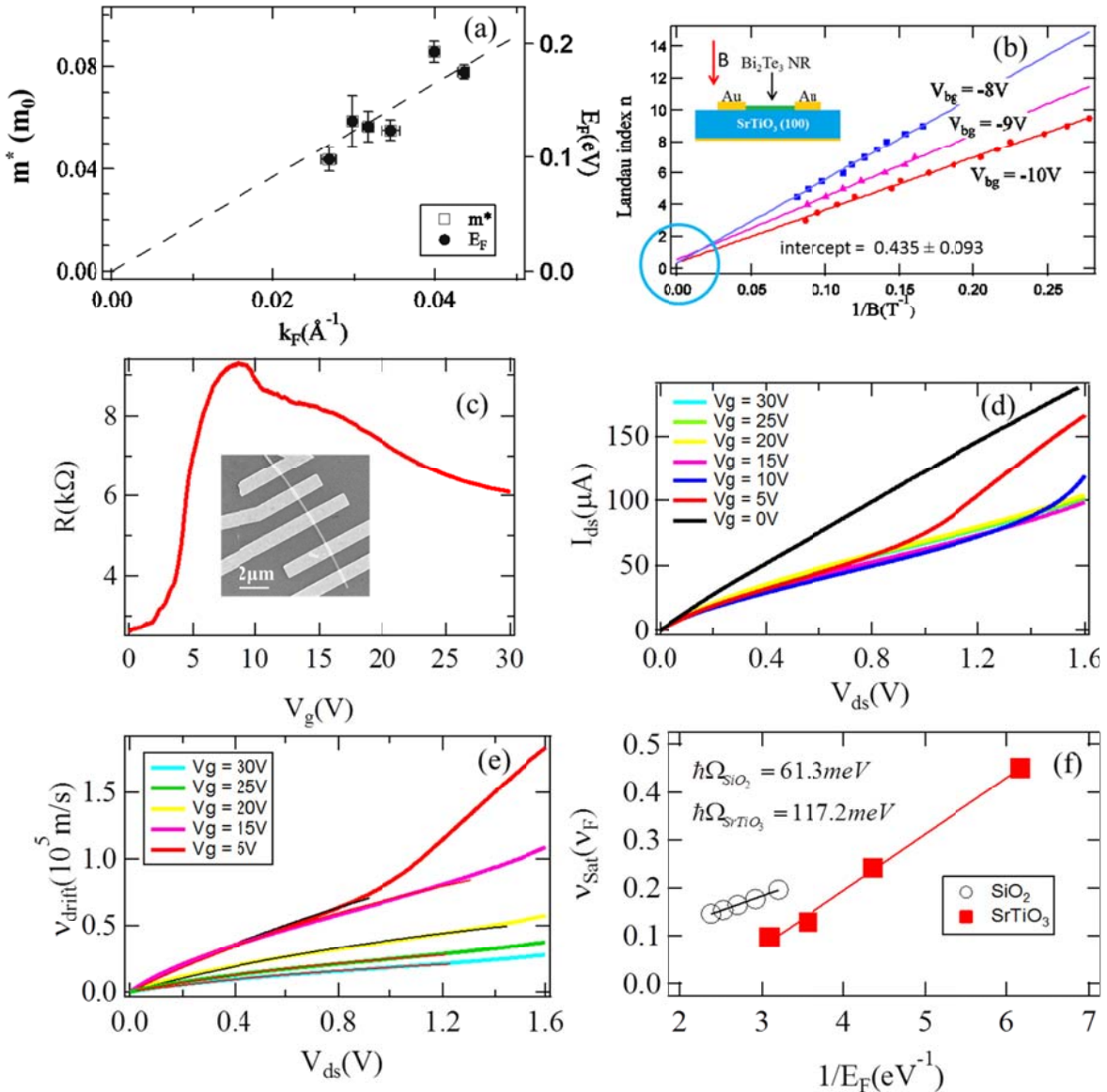


Fig. 1. (a) Effective mass ( $m^*$ ) as well as Fermi energy ( $E_F$ ) vs. Fermi momentum ( $k_F$ ). (b)  $1/B$  vs. Landau level index (fan diagram) at 3 representative  $V_g$ 's. The linear  $E_F$  vs  $k_F$  and the non-zero intercept in the fan diagram are strong signatures of Dirac fermions on the surface of our  $\text{Bi}_2\text{Te}_3$  NWs. Field effect of a  $\text{Bi}_2\text{Te}_3$  TINW ( $L = 1.3 \mu\text{m}$ ,  $W = 0.33 \mu\text{m}$ ) on  $500\mu\text{m}$   $\text{SrTiO}_3$  substrate at  $T = 1.7\text{K}$ . (c) 4-terminals resistance ( $R$ ) vs.  $V_g$ . Inset: SEM picture of such device, scale bar:  $2\mu\text{m}$ . (d) 4-terminals  $I_{ds}$ - $V_{ds}$  curve at 7 representative  $V_g$ 's. (e) Extracted drift velocity ( $v_{drift}$ ) vs.  $V_{ds}$  at 5 representative  $V_g$ 's. Black lines are fitting curves to:  $v_{drift} = ((\mu E)^{-\beta} + (v_{sat})^{-\beta})^{-1/\beta}$ , where  $\mu$  is mobility,  $E$  is electric field,  $v_{sat}$  is the saturation velocity and  $\beta$  is a fitting parameter. (f) Extracted  $v_{sat}$  vs.  $1/E_F$  for TINW devices on  $100\text{nm}$   $\text{SiO}_2$  and  $500 \mu\text{m}$  thick  $\text{SrTiO}_3$  substrates. From the slope, the energy of the interfacial phonons ( $\hbar\Omega$ ) is extracted. For  $\text{SiO}_2$ , the extracted  $\hbar\Omega$  is in good agreement with the surface phonon of  $\text{SiO}_2$ .